Introduction to SLOPE-ffdm 2.0

Ching-Chuan Huang

Professor Emeritus
Department of Civil Engineering,
National Cheng Kung University, Tainan, Taiwan
Email: samhcc@mail.ncku.edu.tw
2025/09/03

1.1 BACKGROUND OF FFDM

For over a century, the limit equilibrium method (LEM) has been a fundamental approach in engineering analyses and design for soil structures. Slope stability assessments using LEM are traditionally expressed through the safety factor (F_s), defined as the ratio of shear strength to shear stress along the slip surface. While F_s has long been used as an indicator of slope stability, it presents inherent limitations that hinder comprehensive analysis and design:

1. Displacements of the slope remain unknown.
2. The definition of F_s relies on the assumption of a single, uniform F_s along the slip surface.

Consequently, F_s serves as a **semi-quantitative** rather than a strictly **quantitative** indicator, making slope stability assessments less straightforward and heavily reliant on empirical judgment.

To address these limitations, Huang (2013) developed the **Force-equilibrium-based Finite Displacement Method (FFDM)**, modifying classical LEM approaches—including those by Fellenius, Bishop, Janbu, Spencer, and the multi-wedge method—to incorporate a more comprehensive analytical framework.

Footsteps of FFDM

The development of the Force-Equilibrium-Based Finite Displacement Method (FFDM) has progressed through a series of peer-reviewed studies, each contributing to its formulation, validation, and extension to various geotechnical scenarios:

1. **Huang, C.-C. (2013)** *Developing a new slice method for slope displacement analyses*, *Engineering Geology*, 157, 39–47.

   — This study introduced the original formulation of FFDM using Janbu's slice method and verified its applicability through a landslide case study.

2. **Huang, C.-C. (2014)** *Force-equilibrium-based finite displacement analyses for reinforced slopes: Formulation and verification*, *Geotextiles and Geomembranes*, 42, 394–404.

— FFDM was first applied to reinforced slopes. Unlike conventional methods where reinforcement force is an input and displacement is unknown, FFDM outputs both slope displacement and mobilized reinforcement force.

3. **Huang, C.-C. and Yeh, S.-W. (2015)** *Predicting periodic rainfall-induced slope displacements using force-equilibrium-based finite displacement method*, *Journal of GeoEngineering*, 10(3), 83–89.

   — Bishop's method was incorporated into FFDM to analyze a landslide in central Taiwan. The study demonstrated that soil parameters back-calculated from an initial displacement event could be used to predict long-term slope movements.

4. **Huang, C.-C. (2016)** *Back-calculating strength parameters and predicting displacements of deep-seated sliding surface comprising weathered rocks*, *International Journal of Rock Mechanics and Mining Sciences*, 88, 98–104.

   — This work verified FFDM's versatility in using different failure criteria, including Mohr-Coulomb and Hoek-Brown. It proved FFDM effective for back-calculating strength and deformation characteristics of slope materials.

5. **Lo, C.-L. and Huang, C.-C. (2021)** *Displacement analyses for a natural slope considering post-peak strength of soils*, *GeoHazards*, 2, 41–62. https://doi.org/10.3390/geohazards2020003 — Introduced a post-peak soil strength model using the "Versoria" curve (also known as the witch of Agnesi), originally developed in Chiang (2017). Combined with hyperbolic pre-peak stress-displacement relationships, this model provided deeper insight into landslide failure processes.

6. **Lo, C.-L. and Huang, C.-C. (2021)** *Groundwater-table-induced slope displacement analyses using different failure criteria*, *Transportation Geotechnics*, 26, 100444. https://doi.org/10.1016/j.trgeo.2020.100444

   — Verified FFDM's predictive capability using back-calculated parameters from groundwater-induced slope movements. Demonstrated FFDM's applicability to both soil and rock slopes using Mohr-Coulomb and Hoek-Brown criteria.

This report, *FFDM Software Development Series 1*, outlines the key features, advantages, and limitations of FFDM. Additionally, three fundamental components forming the FFDM framework are introduced in Sections 1.4 to 1.6:

1. **Stress-displacement constitutive law of soils**
2. **Force and moment equilibria for the entire sliding mass**
3. **Displacement compatibility of the sliding soil mass**

1.2 ADVANTAGES OF FFDM

To evaluate the stability and displacement of natural and engineered slopes, the **Force-equilibrium-based Finite Displacement Method (FFDM)** offers distinct advantages over traditional stability analysis methods:

1. **Displacement Indicators** – FFDM provides both vertical settlement at the crest and shear displacements along the critical failure surface, offering a displacement-based indicator essential for slope stability assessment.
2. **Localized Safety Factors** – Instead of a single lumped safety factor for the entire slip surface, FFDM calculates local displacement-based and stress-based safety factors along the failure surface, enhancing analytical precision.
3. **Computational Efficiency** – FFDM computes slope displacements with minimal additional time and effort compared to conventional slope stability analysis methods. The computer time for analyzing slope displacements using non-linear (hyperbolic) stress-displacement relationships is comparable to that of traditional limit equilibrium calculations for a constant safety factor.
4. **Shear Stress-Displacement Modeling** – FFDM employs a shear stress-displacement relationship akin to that in the discrete element method (DEM), where stress-displacement relationships determine normal and shear spring constants under small displacement conditions. However, FFDM extends this capability to account for larger shear displacements.
5. **Incremental & Cumulative Displacements** – FFDM incorporates the concept of **incremental** and **cumulative** slope displacements, enabling analysis between different internal or external loading states.
6. **Application to Reinforced (or nailed) and Pre-stress Anchored Slopes** – FFDM is suitable for both unreinforced and reinforced slopes. For reinforced and nailed slopes, the mobilized reinforcement (or nailing) force is included in the analytical output, unlike conventional LEM-based methods.

1.3 LIMITATIONS AND ADDITIONAL REQUIREMENTS IN FFDM:

1. **Prescribed Failure Surfaces** – As in conventional LEM analyses, FFDM requires predefined potential failure surfaces, which may take the form of straight lines, bi-linear wedges, multi-wedges, circles, logarithmic spirals, or combinations of these. In SLOPE-ffdm 2.0, all of the above-mentioned failure surfaces can be analyzed, and the critical surface associated with maximum slope displacement can be identified through a trial-and-error process.
2. **Additional Soil Parameters** – FFDM computes slope displacements using the hyperbolic stress-displacement constitutive law, requiring three additional input soil parameters:
   - **Initial shear stiffness number (*K*)**
   - **Stress-dependency exponent (*n*)**
   - **Peak-to-asymptote strength ratio (R_f)**

3. To account for the post-peak strength deterioration of soils in slope displacement analysis, two additional soil parameters are required:

- **Residual friction angle of soil (φ_{res})**
- **Residual-to-peak displacement ratio (Δ_{ratio})**

Studies aimed at establishing a database for these parameters have been conducted through calibration of slope displacements using field monitoring, direct shear tests, and empirical equations.

1.4 STRESS-DISPLACEMENT CONSTITUTIVE LAW

A hyperbolic equation is employed to model the relationship between normalized shear stress (τ/τ_f) and shear displacement (Δ) along the potential failure surface, as illustrated in **Figure 1.4.1**. This formulation is based on Duncan and Chang (1970) and Huang (2013):

$$\frac{\tau}{\tau_f} = \frac{\Delta}{a + b \cdot \Delta} \qquad (1-4-1)$$

Where:

$$a = \frac{\tau_f}{k_{initial}} \qquad (1-4-2)$$

$$b = R_f \qquad (1-4-3)$$

$$R_f = \frac{\tau_f}{\tau_{ult}} \qquad (1-4-4)$$

Parameter Definitions

$k_{initial}$: Initial shear stiffness of soils

τ_{ult}: Asymptote strength at infinite displacement

τ_f:: Shear strength of soil according to the Mohr-Coulomb failure criterion

R_f: Asymptote strength ratio (= τ_f / τ_{ult})

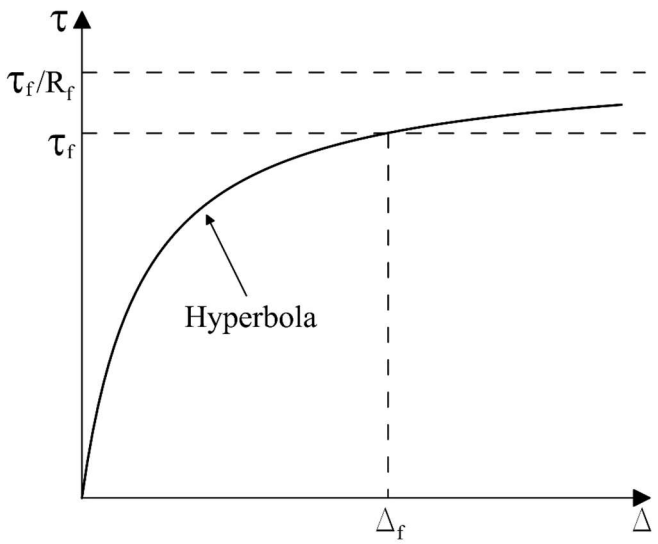

Figure 1.4.1 A hyperbolic normalized stress and shear displacement relationship

The shear strength of soils (τ_f) is defined by the Mohr-Coulomb failure criterion:

$$\tau_f = c + \sigma_n' \cdot \tan\varphi \qquad (1-4-5)$$

σ_n': Effective normal stress

c: Cohesion intercept

φ: Internal friction angle of soils

Equation (1-4-1) can be viewed as a reciprocal formulation of the local safety factor **Fs** at the base of a slice (or wedge) - structurally inverted with respect to **Eq. (1-4-6)**.

$$F_s = \frac{\tau_f}{\tau} \qquad (1-4-6)$$

The initial shear stiffness $k_{initial}$ is given as a power function of effective normal pressure, per Duncan and Chang (1970):

$$k_{initial} = K \cdot G \left(\frac{\sigma'_n}{P_a}\right)^n \qquad (1-4-7)$$

- K: initial shear stiffness number (dimensionless)
- P_a: atmospheric pressure (= 101.3 kPa)
- G: reference shear stiffness (= 101.3 kPa/m)
- n: pressure dependency exponent

Validation and Application

Equations (1-4-1) through (1-4-7) have been validated across multiple soil types using medium- to large-scale direct shear tests. A curve-fitting methodology was employed to establish empirical consistency. Full details will be discussed in the **FFDM Software Development Series 10: Modelling material behavior**.

About Post-Peak Behavior of Soils

A novel modeling approach leverages a classical mathematical curve known as the *Versoria*—also referred to as the *Witch of Agnesi*—originally proposed by Grandi in the 1700s. This curve provides a promising framework for simulating the post-peak strength degradation of soils. The theoretical foundation and simulation results are detailed in **Series 11: Modelling Post-Peak Behavior of Soils**.

1.5 Force and Moment Equilibria in Slope Stability Analysis

This section provides a brief overview of force and moment equilibria considered in various types of analyses. Detailed formulations will be presented in an upcoming series of reports. In slope stability formulations for a potential sliding mass with slices, three types of force and moment equilibrium are adopted:

1. **Circular Failure Surface** – As shown in Fig. 1.5.1, methods such as Fellenius' method (Fellenius, 1936) and Bishop's method (Bishop, 1955) belong to this category. These approaches formulate vertical force equilibrium (or equilibrium normal to the slice base) and overall moment equilibrium for the circular sliding mass.

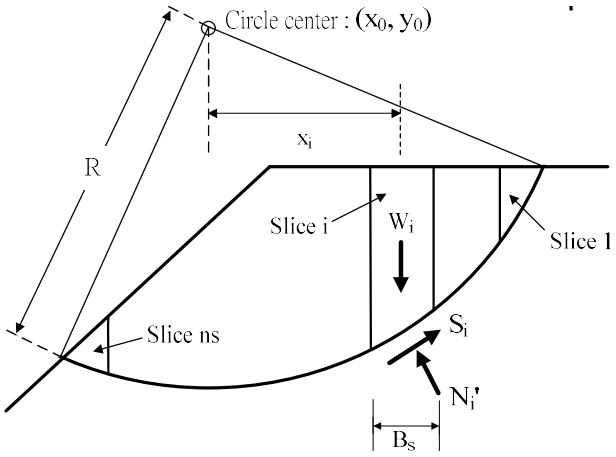

Fig. 1.5.1 A potential failure mass confined by a circular failure surface

2. **Non-Circular Failure Surface** – As shown in Fig. 1.5.2, the rigorous Janbu's method (Janbu, 1973) and Spencer's method (Spencer, 1973) fall into this category. These methods establish force equilibrium in both vertical and horizontal directions and moment equilibrium for each slice within the sliding mass. In the simplified Janbu's method, however, only vertical and horizontal force equilibria are formulated.

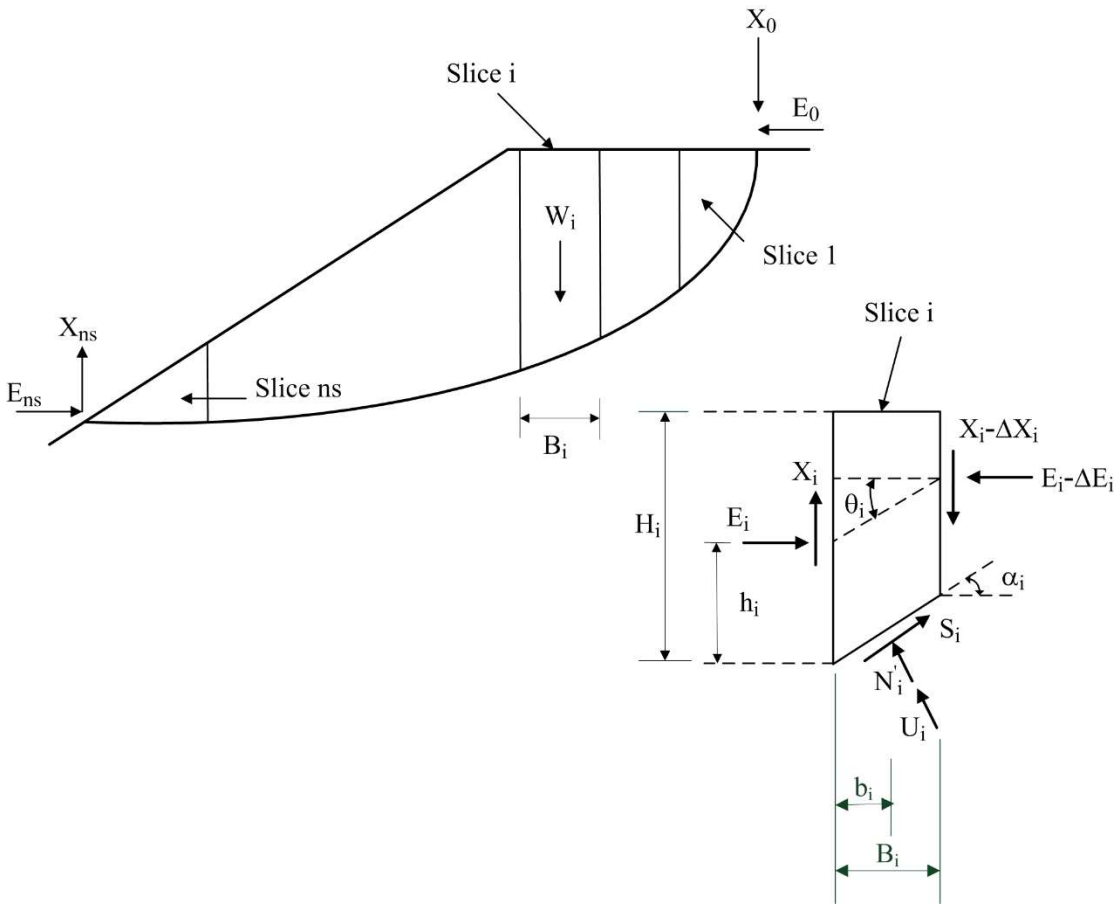

Fig. 1.5.2 Body and reactional forces in a sliced non-circular failure mass

3. **Wedge-Like Failure Surface** – As shown in Fig. 1.5.3, the Multi-wedge method (Huang et al., 2003) and the simplified Janbu's method belong to this category. These methods formulate only force equilibrium in vertical and horizontal directions, without explicitly considering moment equilibrium.

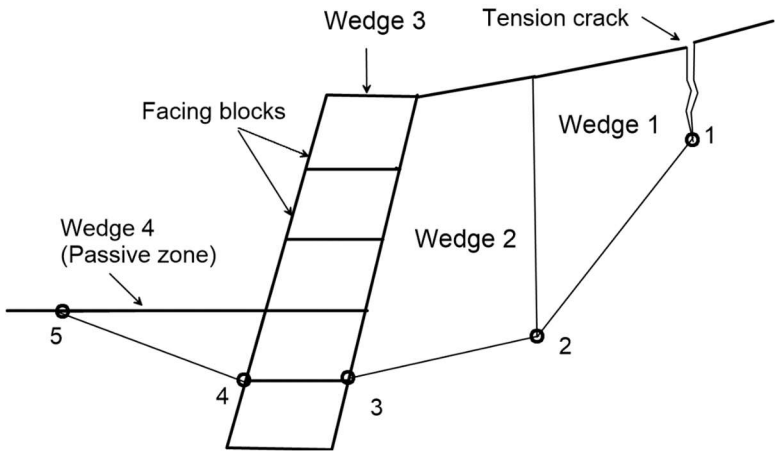

Fig. 1.5.3 Schematic wedge-like failure mass

1.6 DISPLACEMENT COMPATIBILITY

A hodograph (displacement diagram) that satisfies ***displacement compatibility*** - as schematically illustrated in **Figure 1.6.1** - is derived following Atkinson (1981). The shear displacement between adjacent slices (or wedges) is recursively governed by:

$$\Delta_2 = \Delta_1 \cdot \frac{\cos(\alpha_1 - 2\psi)}{\cos(2\psi - \alpha_2)} = \frac{\Delta_0}{\sin(\alpha_1 - \psi)} \cdot \frac{\cos(\alpha_1 - 2\psi)}{\cos(2\psi - \alpha_2)} \qquad (1-6-1)$$

Where:

ψ : Angle of the dilatancy of soils.

For general cases where ***i*** > 2, the displacement at slice ***i*** can be expressed as:

$$\Delta_i = \Delta_{i-1} \cdot \frac{\cos(\alpha_{i-1} - 2\psi)}{\cos(2\psi - \alpha_i)} = \frac{\Delta_0}{\sin(\alpha_1 - \psi)} \cdot \frac{\cos(\alpha_1 - 2\psi)}{\cos(2\psi - \alpha_2)} \cdot \frac{\cos(\alpha_2 - 2\psi)}{\cos(2\psi - \alpha_3)} \cdots\cdots\cdots \cdot \frac{\cos(\alpha_{i-1} - 2\psi)}{\cos(2\psi - \alpha_i)} \qquad (1-6-2)$$

Notably, the following identity holds due to symmetry of the cosine function:

$$\cos(2\psi - \alpha_2) = \cos(\alpha_2 - 2\psi) \qquad (1-6-3)$$

Thus, the general displacement expression can be condensed as:

$$\Delta_i = \Delta_0 \cdot f(\alpha_i) \qquad (1-6-4)$$

Where:

$$f(\alpha_i) = \frac{1}{\sin(\alpha_1 - \psi)} \cdot \frac{\cos(\alpha_1 - 2\psi)}{\cos(2\psi - \alpha_i)} \qquad (1-6-5)$$

This formulation maintains displacement compatibility across soil interfaces and forms the basis for kinematic analysis of the sliding block system.

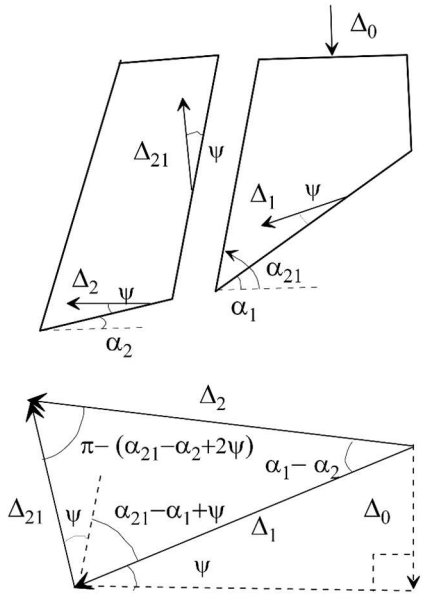

Fig. 1.6.1 Displacement compatibility of adjacent slices

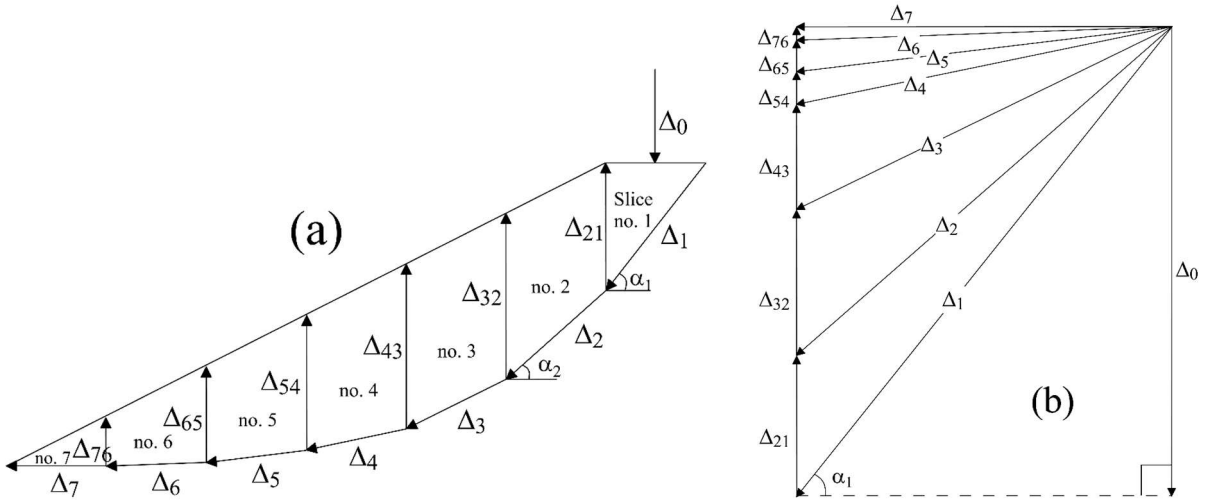

Figure 1.6.2 A constant-volume (Ψ=0) sliding mass with (a) Displacement vectors at the base of slice; (b) Hodograph of the sliding mass

Figure 1.6.2(a) schematically illustrates a constant-volume state of the sliding mass, defined by a dilation angle of $\Psi = 0$. Under this condition, the shear displacement vector at the base of each slice is oriented parallel to the slice base. The corresponding hodograph for the $\Psi = 0$ case is shown in Figure 1.6.2(b), revealing a uniform horizontal displacement component across all slices.

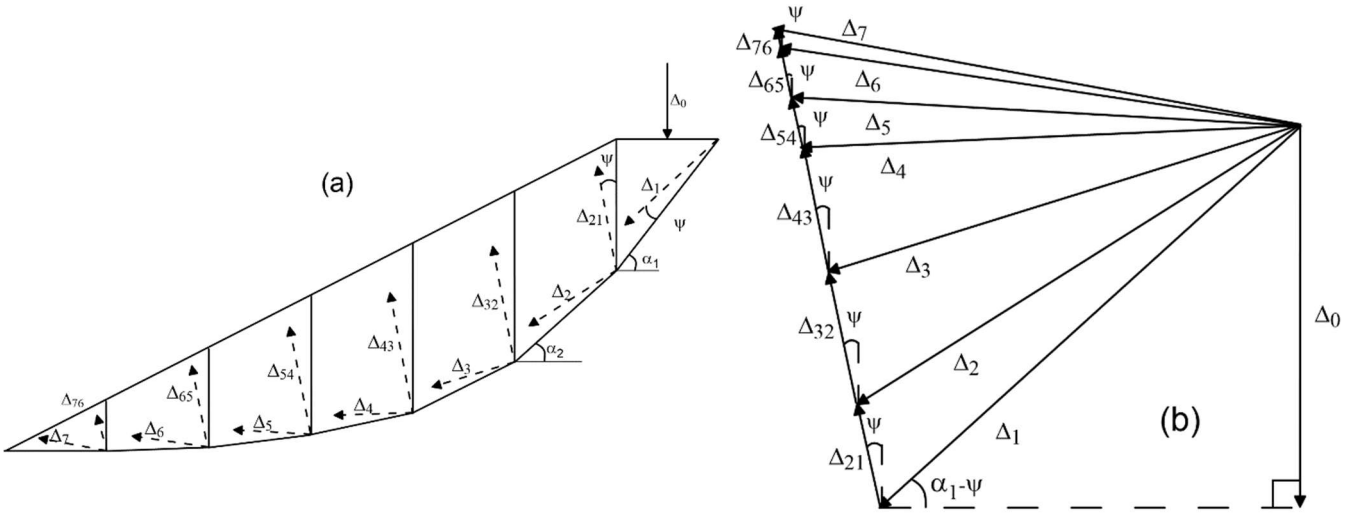

Figure 1.6.3 A constant-volume (Ψ >0) sliding mass with (a) Displacement vectors at the base of slice; (b) Hodograph of the sliding mass

Figure 1.6.3(a) schematically illustrates a dilative state of the sliding mass, characterized by a dilation angle $\Psi > 0$. In this condition, the shear displacement vector at the base of each slice forms an angle Ψ with the slice base. Figure 1.6.3(b) presents a corresponding hodograph for the $\Psi > 0$ case. It reveals that shear displacements along the potential sliding surface progressively increase toward the toe of the slope when dilation is present.

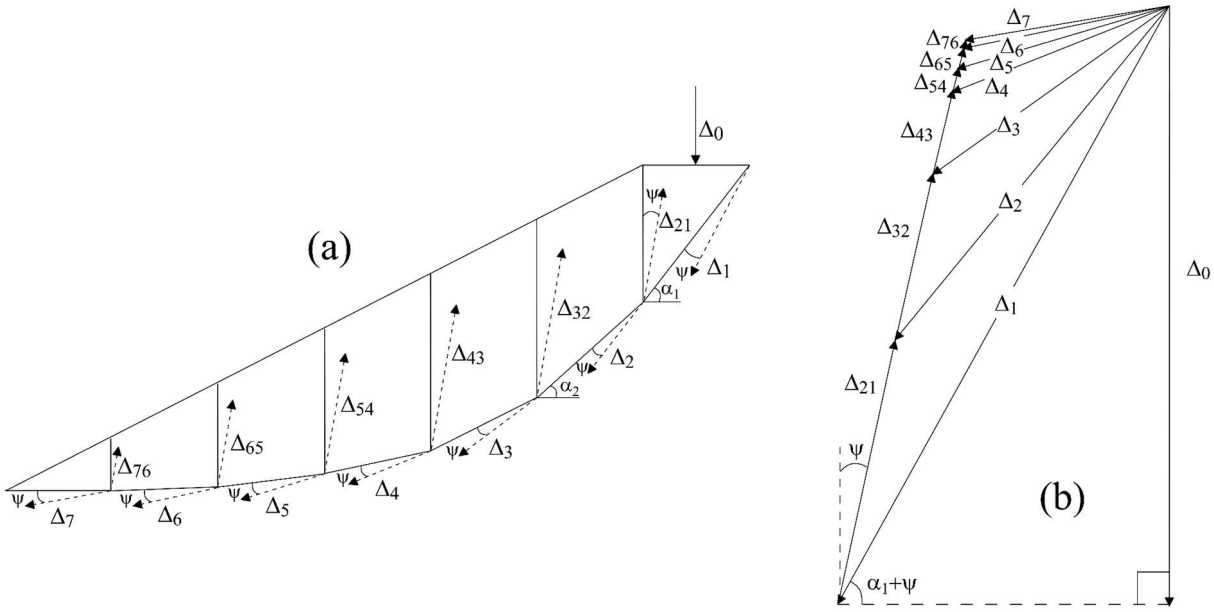

Figure 1.6.4 A constant-volume ($\Psi < 0$) sliding mass with (a) Displacement vectors at the base of slice; (b) Hodograph of the sliding mass

Figure 1.6.4(a) schematically shows the case of dilation (or expansion) of the sliding mass, namely $\Psi < 0$, the vector of shear displacement at the base of the slice has an angle of dilation (Ψ) with the base of slice. A hodograph for the case of $\Psi < 0$ is shown in Fig. 1.6.4(b).

1.7 DISPLACEMENT INCREMENT

To evaluate slope displacements resulting from changes in external or internal conditions—such as loading, variations in the water table, or pore water pressure—two displacement values for each slice (Δ_i) are calculated: one representing the state prior to the event $\left(\Delta_i^a\right)$ and the other representing the state afterward $\left(\Delta_i^b\right)$. The displacement increments for slice ***i***, induced by the change in stress conditions, is schematically illustrated in Figure 1.7.1 and defined as:

$$\Delta_i = \Delta_i^b - \Delta_i^a \qquad (1-7-1)$$

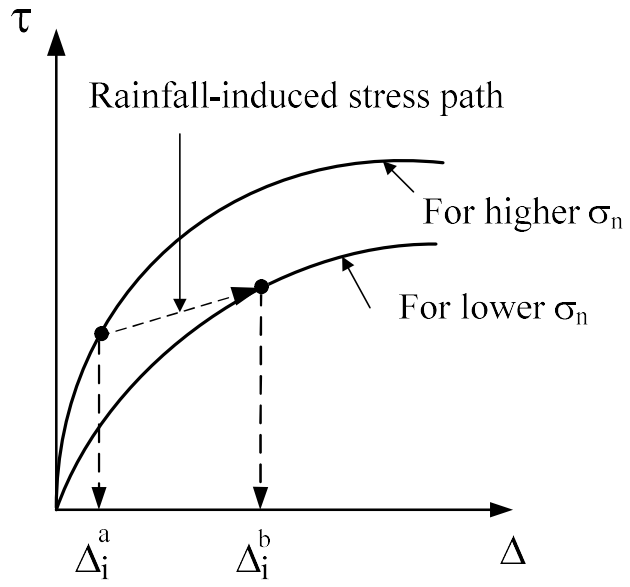

Fig. 1.7.1 Possible shear stress and displacement increases induced by a coupled shear and confining stress increases

REFERENCE

Atkinson, J.H. (1981) “An introduction to applications of critical state soil mechanics” McGraw-Hill, London.

Bishop, A.W. (1955) “The use of slip circle in the stability analysis of slopes” Geotechnique, Vol. 5, No. 1, pp. 7-17.

Chiang, Y.-J. (2017) "Analyses of rainfall-induced slope displacements taking into account various displacement fields and failure criteria" Master thesis of National Cheng Kung University, Tainan, Taiwan.

Duncan, J.M. and Chang, C.Y. (1970) “Nonlinear analysis of stress and strain in soils” Journal of the Soil Mechanics and Foundation Division, ASCE, Vol. 96, No. SM5, pp. 1629-1653.

Fellenius, W. (1936) “Calculation of the stability of earth dams” Proceedings of 2nd Congress on Large Dams, Vol. 4, pp. 445-463.

Huang, C.-C. (2013) “Developing a new slice method for slope displacement analyses” Engineering Geology, Vol. 157, pp. 39-47.

Huang, C.-C., Chou, L.H. and Tatsuoka, F. (2003) “Seismic displacements of geosynthetic-reinforced soil modular block walls” Geosynthetics International, Vol. 10, No. 1, pp. 2-23.

Janbu, N. (1973) Slope stability computation, Embankment-Dam Engineering, Casagrande Volume, John Wiley & Sons, pp. 47-86.

Spencer, E. (1973) “Thrust line criterion in embankment stability analysis” Geotechnique, Vol. 23, No. 1, pp. 85-100.